PHOTONICS Research

All-fiber acousto-optic modulator based on a cladding-etched optical fiber for active mode-locking

Jihwan Kim, Joonhoi Koo, and Ju Han Lee*

School of Electrical and Computer Engineering, University of Seoul, 163 Seoulsiripdae-ro, Dongdaemun-gu, Seoul 02504, South Korea
*Corresponding author: j.h.lee@ieee.org

Received 9 May 2017; revised 9 July 2017; accepted 9 July 2017; posted 10 July 2017 (Doc. ID 295568); published 11 August 2017

An all-fiber acousto-optic modulator (AOM), which features a compact structure and a low-driving voltage, is experimentally demonstrated for the active mode-locking of a fiber laser. The proposed AOM is based on the short length of the cladding-etched fiber, the ends of which are fixed on a slide glass. On top of the cladding-etched fiber, a piezoelectric transducer was overlaid. A chemical wet-etching technique, which is based on a mixed solution of NH_4F and $(NH_4)_2SO_4$, is used to reduce the fiber diameter down to ~25 μm, and the length of the etched section is only 0.5 cm. The fabricated device exhibited a modulation depth of 73.10% at an acoustic frequency of 918.9 kHz and a peak-to-peak electrical voltage of 10 V, while a laser beam was coupled at 1560 nm. By using the prepared AOM within an erbium-doped-fiber ring cavity, the mode-locked pulses with a temporal width of 2.66 ps were readily obtained at a repetition rate of 1.838 MHz. © 2017 Chinese Laser Press

OCIS codes: (060.2340) Fiber optics components; (140.4050) Mode-locked lasers; (230.1040) Acousto-optical devices.

https://doi.org/10.1364/PRJ.5.000391

1. INTRODUCTION

Mode-locked fiber lasers have been a useful light source for a range of applications such as high-speed optical communications, biomedical imaging, and material processing [1–3]. Mode-locking can be obtained with either passive or active techniques. Passive mode-locking is usually implemented using a saturable absorber (SA) within a laser cavity, even if the passive mode-locking has several advantages over the active mode-locking (for example, regarding a simple configuration without the need of an external electrical-signal source and the easy generation of subpicosecond optical pulses), the drawbacks are that the flexible control of the repetition rate and the external synchronization are not readily achieved. Alternatively, active mode-locking is implemented by the external modulation of the intracavity loss or the round-trip phase. The output pulses generated from the active mode-locking schemes have a lower phase noise because each output pulse is triggered by an external electrical-signal generator. The main drawback of active mode-locking, however, is the relatively large temporal width of the output optical pulses at low repetition rates. The commonly used active-modulation devices are the electro-optic modulators (EOMs) or the acousto-optic modulators (AOMs).

In the field of the actively mode-locked fiber lasers, one of the technically interesting issues is the way that the all-fiberized configurations are achieved without the use of bulk modulators such as the conventional EOMs or AOMs [4–14]. Until now, a fair number of investigations have been conducted into the use of an optical fiber-based modulator as a mode-locker, and they have been conducted because they allow for a range of advantages such as a low insertion loss and a large optical-damage threshold; here, the modulators are based on the acousto-optic modulation effect within an optical-fiber medium [5]. Conventional optical-fiber-based AOMs consist of a high-voltage electrical-signal source, a piezoelectric transducer (PZT), a horn, and a small section of uncoated optical fiber [4,5]. Recently, it was demonstrated by Bello-Jiménez *et al.* that soliton pulses with a temporal width as short as 25 ps could readily be produced at a repetition rate of 2.46 MHz with a ~23 cm long tapered fiber-based AOM [13]. Even if such an AOM, which is based on long tapered-fiber length, allows for a high modulation depth and a broad bandwidth, the issue of a bulky and sophisticated configuration that is vulnerable to environmental fluctuations needs to be addressed.

In this paper, a simple and compact all-fiber AOM, which can be readily used for the active mode-locking of a fiber laser, is experimentally demonstrated. The proposed modulator is based on a simple combination of short-length cladding-etched fiber and a PZT, unlike the conventional ones based on a large-size horn and a long-length uncoated optical fiber [11–13]. More specifically, a PZT is simply placed on top of a 0.5 cm long cladding-etched section of a bare fiber to construct

an AOM. A chemical wet-etching technique, which has been proposed in Ref. [15], was used to reduce the fiber diameter down to ~25 μm. The fabricated device exhibited a modulation depth of 73.10% at an acoustic frequency of 918.9 kHz and a peak-to-peak electrical voltage of 10 V when a laser beam at 1560 nm was coupled. Using the prepared AOM within an erbium-doped-fiber (EDF) ring cavity, the mode-locked pulses with a temporal width of 2.66 ps were readily obtained at a repetition rate of 1.838 MHz.

Compared with the previously demonstrated optical-fiber-based AOMs [11–13], the technically distinguishable features of the proposed AOM are as follows: First, a standing acoustic flexural wave was produced through the application of a uniform pressure along with the cladding-etched fiber, rather than an application into one end of a long-length bare or tapered fiber; second, a large-size horn was not used; third, the entire structure is compact because a short length of the cladding-etched optical fiber was used. The lengths of the bare or tapered optical fiber for the previously demonstrated optical fiber-based AOMs are no less than 20 cm [11,13]. Fourth, the peak-to-peak voltage of the electrical-signal voltage, which was applied to the PZT, is much smaller than the values of the conventional fiber-optic AOMs [13].

2. ACOUSTO-OPTIC MODULATOR BASED ON CLADDING-ETCHED FIBER

The AOM schematic based on the double-ended cladding-etched fiber is shown in Fig. 1(a), and the magnified side-view of the AOM is shown in Fig. 1(b). The AOM consists of a radio frequency (RF) source, a PZT, and a double-ended cladding-etched fiber.

The cladding-etched fiber was prepared using a mixed solution of NH_4F and $(NH_4)_2SO_4$, which was contained within a small etching cradle for approximately 6 h. Further details on

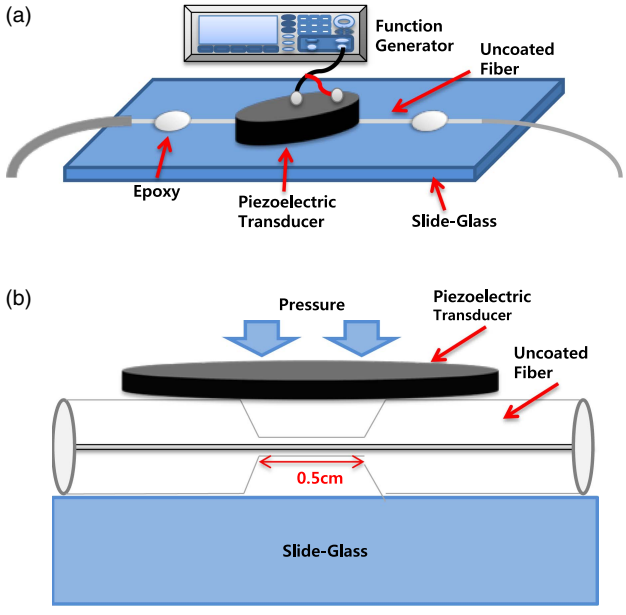

Fig. 1. (a) Experimental setup of the proposed AOM. (b) Its magnified side-view.

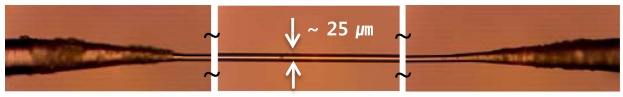

Fig. 2. Microscopic images of the etched optical fiber.

the wet-etching technique are fully described in Ref. [15]. For the etching process, an HF solution also could be used [16]. The fiber diameter was reduced down to ~25 μm by the wet etching, and the length of the cladding-etched fiber section is only 0.5 cm. The polarization dependence loss of the etched optical fiber was measured at ~0.05 dB at 1550 nm. The microscopic images of the etched optical fiber are shown in Fig. 2.

The cladding-etched fiber was placed on a slide glass. Both ends of the cladding-etched optical fiber were clamped with epoxy to produce a standing acoustic wave, as shown in Fig. 1(a). The PZT was then placed on top of the cladding-etched fiber, as shown in Fig. 1(b), to convert the input electrical signal into an acoustic wave.

The prepared AOM was characterized in terms of the beam-modulation performance. The modulation depth of the AOM was first measured at a wavelength of 1560 nm, as the applied electrical-signal frequency was changed by a step of 0.5 kHz together with a Lorentzian-fitting curve, as shown in Fig. 3(a). For this measurement, the peak-to-peak voltage of the electrical signal, which was applied to the PZT, was set at 10 V. The maximum modulation depth of 73.1% was observed at an

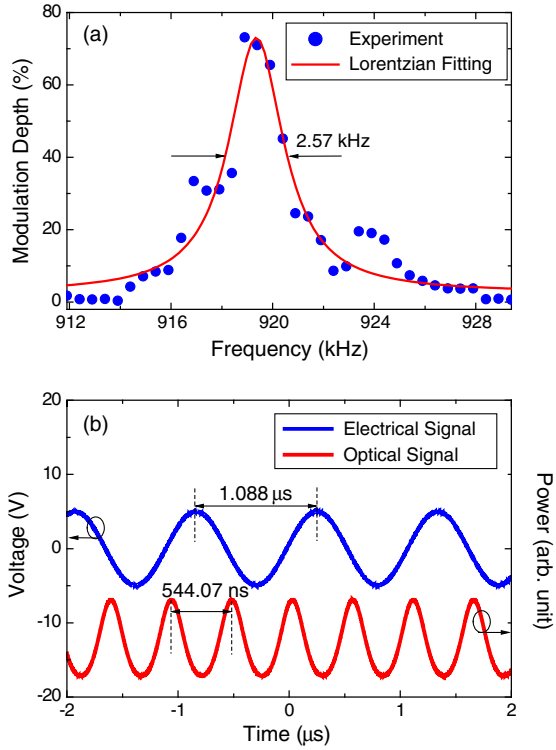

Fig. 3. (a) Measured modulation depth as a function of the electrical frequency at the wavelength of 1560 nm. (b) Measured oscilloscope traces of the applied electrical signal to the prepared AOM and the output optical signal.

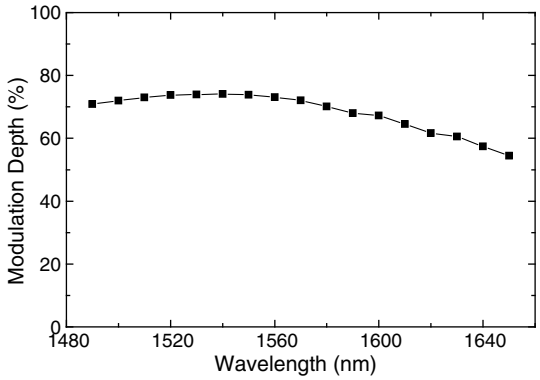

Fig. 4. Measured modulation depth as a function of the input-beam wavelength when the frequency and the peak-to-peak amplitude of the electrical signal, which was applied to the PZT, were fixed at 918.9 kHz and 10 V, respectively.

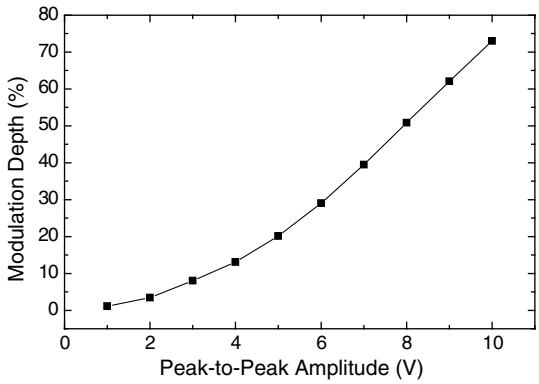

Fig. 5. Measured modulation depth as a function of the peak-to-peak amplitude of the electrical signal applied to the PZT. Both the electrical signal frequency and the wavelength of the input laser beam were fixed at 918.9 kHz and 1560 nm, respectively.

electrical-signal frequency of 918.9 kHz. From the fitting curve, the FWHM of the frequency response of the modulation depth was estimated as 2.57 kHz. Figure 3(b) shows the measured oscilloscope traces of the electrical signal, which was used to drive the PZT together with a modulated optical beam. It is obvious from the figure that the frequency of the modulated beam (1.838 MHz) is twice as large as that of the electrical signal (918.9 kHz). The frequency doubling can be attributed to the formation of a standing acoustic wave [12,17].

Figure 4 shows the modulation depth versus the input-beam wavelength. The wavelength of the input laser beam was changed from 1490 to 1650 nm by a 10 nm step, while the frequency and peak-to-peak amplitude of the electrical signal, which were applied to the PZT, were fixed at 918.9 kHz and 10 V, respectively. The maximum modulation depth of ~74% was observed at a wavelength of 1540 nm. Interestingly, a non-negligible modulation depth (54%) is still evident at 1650 nm. The maximum modulation depth was observed at a wavelength of ~1490 nm when the electrical frequency is 922.4 kHz. The wavelength for the maximum modulation depth was observed to shift to a shorter wavelength when the electrical frequency was enlarged.

The measured FWHM of the modulation-depth spectrum must be larger than 170 nm, as shown in Fig. 4; notably, the proposed modulation-depth spectrum measurement as a function of the input-beam wavelength is limited due to the wavelength-tuning bandwidth of the tunable laser, which was used for this particular measurement. The reason why such a broad operating bandwidth was readily obtained with our prepared AOM should be associated with the significantly reduced cladding thickness without change of the core size as well as ultra-short acousto-optic interaction length. Note that it was previously reported by Li *et al.* that both the acousto-optic coupling efficiency and the corresponding optical bandwidth are enhanced when the outer cladding diameter of an optical fiber is reduced [18]. Furthermore, it was also reported that the optical bandwidth of fiber-optic acousto-optic device is inversely proportional to the interaction length between the acoustic wave and the optical beam as follows [18,19]:

$$\Delta\lambda = \frac{0.8\pi}{L\left(\frac{\partial\beta_{01}}{\partial\lambda} - \frac{\partial\beta_{1n}}{\partial\lambda}\right)}, \tag{1}$$

where λ is the wavelength of the light, L is the length of the coupling region, β_{01} and β_{1n} are the propagation constants of the core mode and the cladding mode. Note that Jin *et al.* demonstrated an optical bandwidth of 360 nm using an etched optical fiber with a diameter of 21 μm and a length of 2.2 cm. However, the AOM demonstrated in Ref. [13] used a tapered fiber with a diameter of 80 μm and a length of 23.7 cm, which resulted in an optical bandwidth of 13 nm.

Then, we measured modulation depth as a function of the peak-to-peak amplitude of the electrical signal, which was applied to the PZT, while both the electrical signal frequency and the wavelength of the input laser beam were fixed at 918.9 kHz and 1560 nm, respectively. It was clearly observed that the modulation depth increased with an increasing electrical signal amplitude, as shown in Fig. 5.

3. MODE-LOCKED FIBER LASER

To check the applicability of the proposed AOM for the fiber-laser mode-locking, a simple fiberized ring cavity was constructed, as shown in Fig. 6. A 3.9 m long EDF with a peak

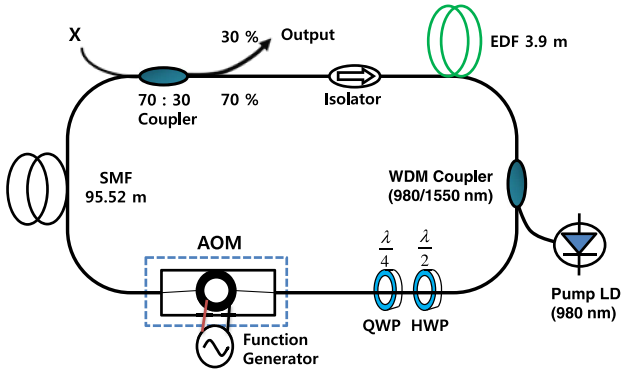

Fig. 6. Experimental schematic of the mode-locked fiber laser for which the prepared AOM was incorporated.

absorption of 13 dB/m at 1530 nm was used as a gain medium; it was pumped by a 980 nm laser diode (LD), and it provides a maximum pump power of 400 mW via a 980/1550 nm wavelength division multiplexer (WDM) coupler. An isolator and a polarization controller (PC), based on the combination of a quarter-wave plate (QWP) and a half-wave plate (HWP), were used to ensure a unidirectional operation and for the polarization adjustment, respectively. The AOM was inserted after the PC. The insertion loss of the fiberized AOM was measured at ~0.61 dB only. The 95.52 m length of the standard single-mode fiber (SMF) was inserted with the cavity to ensure that the round-trip time is coincident with the reciprocal number of the repetition rate of the modulated optical-beam frequency. The total cavity length is ~112.89 m. The chosen electrical-signal frequency applied to the PZT is 918.911 kHz, and the frequency of the modulated optical beam is ~1.838 MHz. Notably, a fine adjustment of the cavity length was not necessary because the proposed AOM exhibited a modulation depth of ~73% over an electrical-signal band from 918.9 to 919.4 kHz.

Figure 7(a) shows the measured oscilloscope trace of the mode-locked optical pulses at a repetition rate of 1.838 MHz with a pump power of 108 mW; here, it is obvious that stable mode-locked pulses were readily obtained. The measured optical spectrum of the output pulses at a pump power of 108 mW is shown in Fig. 7(b) together with its a secant

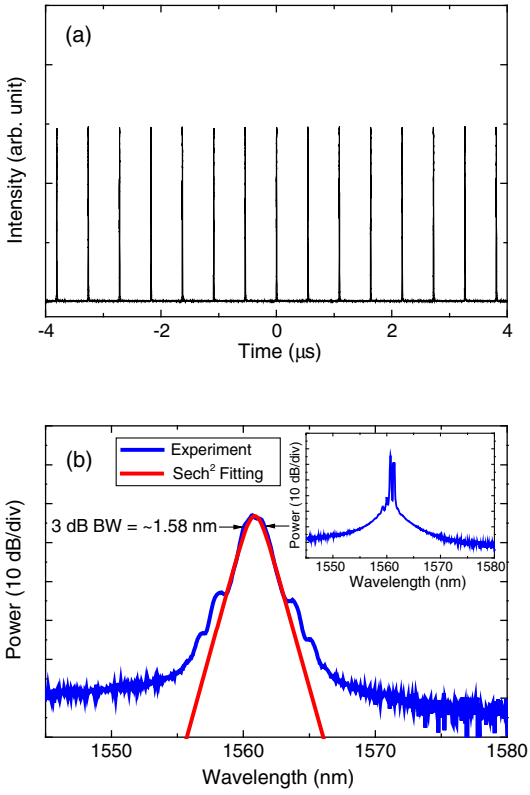

Fig. 7. (a) Measured oscilloscope trace of the output pulses. (b) Measured optical spectrum of the output pulses at a pump power of 108 mW. Inset shows a measured optical spectrum of the output pulses when the electrical signal was off. These measurements were conducted with a pump power of 108 mW.

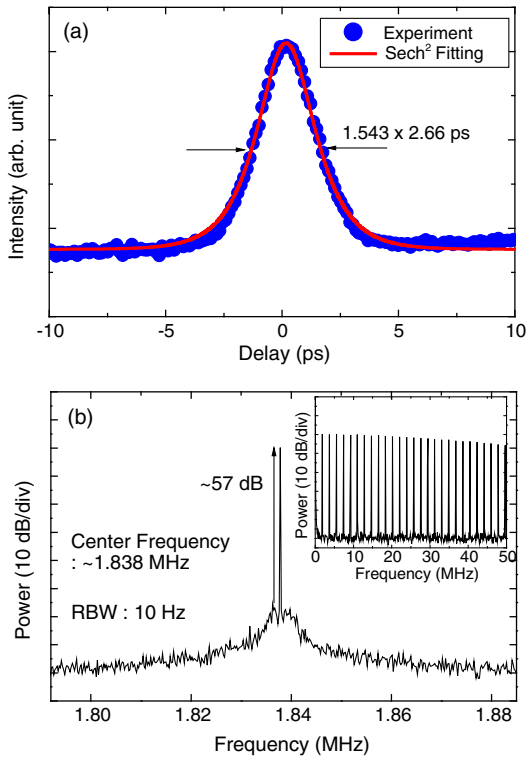

Fig. 8. (a) Measured autocorrelation trace of the output pulses. (b) Measured electrical spectrum of the output pulses. Inset shows a wide-span electrical spectrum. These measurements were conducted with a pump power of 108 mW.

hyperbolic-fitting curve. The center wavelength and the 3 dB bandwidth were measured at ~1560.82 and ~1.58 nm, respectively. The inset of Fig. 7(b) shows the measured optical spectrum of the output pulses when the electrical signal was switched off. The estimated time-bandwidth product is 0.517, which is quite higher than the 0.315 value of the transform-limited sech^2 pulses that indicate that the pulses were largely chirped.

An autocorrelation measurement was then performed using a two-photon absorption-based autocorrelator, and Fig. 8(a) shows the measured curve together with a secant hyperbolic-fitting curve. The pulse width was measured as ~2.66 ps. To the best of the authors' knowledge, until now, the shortest temporal width of the output pulses from the mode-locked fiber lasers, based on optical fiber-based AOMs, is 25.35 ps [13]. It is believed that the reason for the authors' laser generation of such short, mode-locked pulses is associated with the broad- and flat-wavelength modulation bandwidths [20], but it would be difficult to produce femtosecond pulses from our laser configuration due to the limited spectral bandwidth of the output pulses.

Then, the electrical-spectrum measurement of the output pulses was conducted, as shown in Fig. 8(b). A strong signal peak with a fundamental repetition rate of 1.838 MHz was observed, and the peak-to-background ratio was measured as ~57 dB.

Lastly, the peak optical power and the temporal width of the output pulses were measured as a function of the pump power,

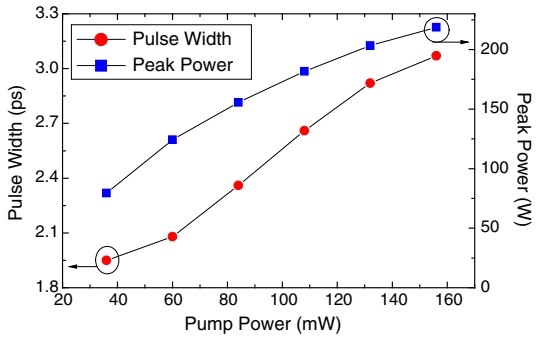

Fig. 9. Measured temporal width and peak power of the output pulses as a function of the pump power.

as shown in Fig. 9. Both the pulse width and the peak power monotonically increased with the increasing of the pump power, as expected [11].

4. CONCLUSION

A simple and compact AOM, which is based on a cladding-etched optical fiber, has been experimentally demonstrated in the present paper. The proposed AOM was implemented through the placement of a PZT on the top of a cladding-etched section of the optical fiber, the ends of which were fixed on a slide glass. The maximum modulation depth of the AOM is 73.1% at an acoustic frequency of 918.9 kHz and a peak-to-peak RF voltage of 10 V. By using the prepared AOM within an EDF ring cavity, stable mode-locked pulses with a temporal width of 2.66 ps were readily achieved at a repetition rate of 1.838 MHz.

The proposed AOM should be applicable as a compact and low-driving-voltage alternative to the conventional micro-optic-based AOMs. To this end, further research must be conducted for the optimization of the AOM performance. We designed the proposed AOM structure from repeated experimental experience. A theoretical investigation into the proposed AOM structure needs to be conducted for the optimization of the device configuration.

Funding. National Research Foundation of Korea (NRF) (2015R1A2A2A04006979, 2015R1A2A2A11000907); Institute for Information and Communications Technology Promotion (IITP-2017-2015-0-00385).

REFERENCES

1. E. Yoshida, N. Shimizu, and M. Nakazawa, "A 40-GHz 0.9-ps regeneratively mode-locked fiber laser with a tuning range of 1530-1560 nm," IEEE Photon. Technol. Lett. **11**, 1587–1589 (1999).
2. H. D. Lee, J. H. Lee, M. Y. Jeong, and C.-S. Kim, "Characterization of wavelength-swept active mode locking fiber laser based on reflective semiconductor optical amplifier," Opt. Express **19**, 14586–14593 (2011).
3. C. B. Schaffer, A. Brodeur, J. F. García, and E. Mazur, "Micromachining bulk glass by use of femtosecond laser pulses with nanojoule energy," Opt. Lett. **26**, 93–95 (2001).
4. M. Y. Jeon, H. K. Lee, K. H. Kim, E. H. Lee, S. H. Yun, B. Y. Kim, and Y. W. Koh, "An electronically wavelength-tunable mode-locked fiber laser using an all-fiber acoustooptic tunable filter," IEEE Photon. Technol. Lett. **8**, 1618–1620 (1996).
5. M. Y. Jeon, H. K. Lee, K. H. Kim, E. H. Lee, W. Y. Oh, B. Y. Kim, H. W. Lee, and Y. W. Koh, "Harmonically mode-locked fiber laser with an acousto-optic modulator in a Sagnac loop and Faraday rotating mirror cavity," Opt. Commun. **149**, 312–316 (1998).
6. D. Culverhouse, D. Richardson, T. Birks, and P. Russell, "All-fiber sliding-frequency Er^{3+}/Yb^{3+} soliton laser," Opt. Lett. **20**, 2381–2383 (1995).
7. N. Myren and W. Margulis, "All-fiber electrooptical mode-locking and tuning," IEEE Photon. Technol. Lett. **17**, 2047–2049 (2005).
8. M. Phillips, A. Ferguson, G. Kino, and D. Patterson, "Mode-locked fiber laser with a fiber phase modulator," Opt. Lett. **14**, 680–682 (1989).
9. C. Cuadrado-Laborde, A. Díez, M. Delgado-Pinar, J. L. Cruz, and M. V. Andrés, "Mode locking of an all-fiber laser by acousto-optic superlattice modulation," Opt. Lett. **34**, 1111–1113 (2009).
10. C. Cuadrado-Laborde, A. Díez, J. L. Cruz, and M. V. Andrés, "Experimental study of an all-fiber laser actively mode-locked by standing-wave acousto-optic modulation," Appl. Phys. B **99**, 95–99 (2010).
11. M. Bello-Jiménez, C. Cuadrado-Laborde, D. Sáez-Rodríguez, A. Díez, J. L. Cruz, and M. V. Andrés, "Actively mode-locked fiber ring laser by intermodal acousto-optic modulation," Opt. Lett. **35**, 3781–3783 (2010).
12. M. Bello-Jiménez, C. Cuadrado-Laborde, A. Díez, J. L. Cruz, and M. V. Andrés, "Experimental study of an actively mode-locked fiber ring laser based on in-fiber amplitude modulation," Appl. Phys. B **105**, 269–276 (2011).
13. M. Bello-Jiménez, C. Cuadrado-Laborde, A. Díez, J. L. Cruz, M. V. Andrés, and A. Rodríguez-Cobos, "Mode-locked all-fiber ring laser based on broad bandwidth in-fiber acousto-optic modulator," Appl. Phys. B **110**, 73–80 (2013).
14. C. Cuadrado-Laborde, M. Bello-Jiménez, A. Díez, J. L. Cruz, and M. V. Andrés, "Long-cavity all-fiber ring laser actively mode locked with an in-fiber bandpass acousto-optic modulator," Opt. Lett. **39**, 68–71 (2014).
15. S. Ko, J. Lee, J. Koo, B. Joo, M. Gu, and J. H. Lee, "Chemical wet etching of an optical fiber using a hydrogen fluoride-free solution for a saturable absorber based on the evanescent field interaction," J. Lightwave Technol. **34**, 3776–3784 (2016).
16. T. Jin, Q. Li, J. Zhao, K. Cheng, and X. Liu, "Ultra-broad-band AOTF based on cladding etched single-mode fiber," IEEE Photon. Technol. Lett. **14**, 1133–1135 (2002).
17. H. S. Kim, S. H. Yun, I. K. Kwang, and B. Y. Kim, "All-fiber acousto-optic tunable notch filter with electronically controllable spectral profile," Opt. Lett. **22**, 1476–1478 (1997).
18. Q. Li, X. Liu, J. Peng, B. Zhou, E. R. Lyons, and H. P. Lee, "Highly efficient acoustooptic tunable filter based on cladding etched single-mode fiber," IEEE Photon. Technol. Lett. **14**, 337–339 (2002).
19. H. E. Engan, B. Y. Kim, J. N. Blake, and H. J. Shaw, "Propagation and optical interaction of guided acoustic waves in two-mode optical fibers," J. Lightwave Technol. **6**, 428–436 (1988).
20. D. J. Kuizenga and A. E. Siegman, "FM and AM mode locking of the homogeneous laser—Part I: Theory," IEEE J. Quantum Electron. **6**, 694–708 (1970).